

DDR complex facilitates global association of RNA polymerase V to promoters and evolutionarily young transposons

Xuehua Zhong^{1,4}, Christopher J Hale^{1,4}, Julie A Law¹, Lianna M Johnson¹, Suhua Feng¹, Andy Tu¹ & Steven E Jacobsen¹⁻³

The plant-specific DNA-dependent RNA polymerase V (Pol V) evolved from Pol II to function in an RNA-directed DNA methylation pathway. Here, we have identified targets of Pol V in *Arabidopsis thaliana* on a genome-wide scale using ChIP-seq of NRPE1, the largest catalytic subunit of Pol V. We found that Pol V is enriched at promoters and evolutionarily recent transposons. This localization pattern is highly correlated with Pol V-dependent DNA methylation and small RNA accumulation. We also show that genome-wide chromatin association of Pol V is dependent on all members of a putative chromatin-remodeling complex termed DDR. Our study presents a genome-wide view of Pol V occupancy and sheds light on the mechanistic basis of Pol V localization. Furthermore, these findings suggest a role for Pol V and RNA-directed DNA methylation in genome surveillance and in responding to genome evolution.

De novo DNA methylation in the *Arabidopsis* genome within all sequence contexts is carried out by the DRM2 DNA methyltransferase via the RNA-directed DNA methylation (RdDM) pathway¹. In contrast, maintenance of DNA methylation is carried out by different DNA methyltransferase systems for cytosines in each of three different sequence contexts. CG and CHG (where H is either C, T or A) are maintained by the MET1 and CMT3 DNA methyltransferases, respectively, whereas asymmetric CHH-context methylation is mostly maintained via persistent targeting by DRM2 and the RdDM pathway^{1,2}.

All eukaryotes have three DNA-dependent RNA polymerases (Pol I, Pol II and Pol III) that are essential for transcription of the genome³. Plants have two additional polymerases (Pol IV and Pol V) that have evolved from Pol II to act in RdDM, wherein small RNAs target *de novo* DNA methylation to transposons and other sequences in the genome^{1,3}. Whereas Pol IV is required for the genome-wide production of 24-nucleotide (nt) small RNAs⁴, Pol V is thought, based on single-locus studies at several intergenic (IGN) loci, to generate non-coding RNA transcripts that serve as molecular scaffolds for recruiting downstream RdDM components⁵.

Several RdDM effectors have been shown to interact with Pol V and assist in its function at various stages of action⁶⁻¹¹. The Argonaute protein AGO4 and the putative elongation factor SPT5L interact with Pol V but act downstream of Pol V binding to chromatin¹²⁻¹⁴. In contrast, a previously identified putative chromatin-remodeling complex termed DDR is thought to act upstream of Pol V to either regulate Pol V activity or stabilize Pol V association with chromatin⁹. The DRD1,

DMS3 and RDM1 proteins comprise the DDR complex, and each was previously shown to be required for the production of Pol V-dependent noncoding RNAs at two IGN regions, IGN5 and MEA-ISR^{5,9,15}. DRD1 and DMS3 were also reported to mediate Pol V recruitment at several IGN loci^{5,15}. However, despite these informative studies, the current RdDM model for Pol V function is largely based on the characterization of the few identified targets of Pol V, and it remains unknown where Pol V is active in the genome, to what extent RdDM components are required for Pol V localization and what might distinguish Pol V targets from nontargets. To address these questions and present what is, to our knowledge, the first profile of genome-wide Pol V occupancy, we performed chromatin immunoprecipitation in combination with massively parallel sequencing (ChIP-seq) in both wild-type and mutant plants. We found that Pol V is enriched at gene promoter regions and evolutionarily young transposons containing marks of epigenetic silencing and that genome-wide Pol V localization is dependent on DDR-complex components.

RESULTS

Pol V occupancy is correlated with epigenetic silencing marks

Using ChIP-seq, we generated a genome-wide map of the chromatin-association profile of NRPE1, the largest catalytic subunit of Pol V, in *Arabidopsis* flowers expressing Flag epitope-tagged NRPE1¹². At the chromosomal level, NRPE1 was enriched in pericentromeric heterochromatin but not at the central core of centromeric regions (Fig. 1a). In addition, we identified 2,600 small NRPE1-enriched regions, distributed throughout the chromosomes, that were reproducible

¹Department of Molecular, Cell and Developmental Biology, University of California, Los Angeles, Los Angeles, California, USA. ²Howard Hughes Medical Institute, University of California, Los Angeles, Los Angeles, California, USA. ³Eli and Edythe Broad Center of Regenerative Medicine and Stem Cell Research, University of California, Los Angeles, Los Angeles, California, USA. ⁴These authors contributed equally to this work. Correspondence should be addressed to S.E.J. (jacobsen@ucla.edu).

Received 28 April; accepted 6 July; published online 5 August 2012; doi:10.1038/nsmb.2354

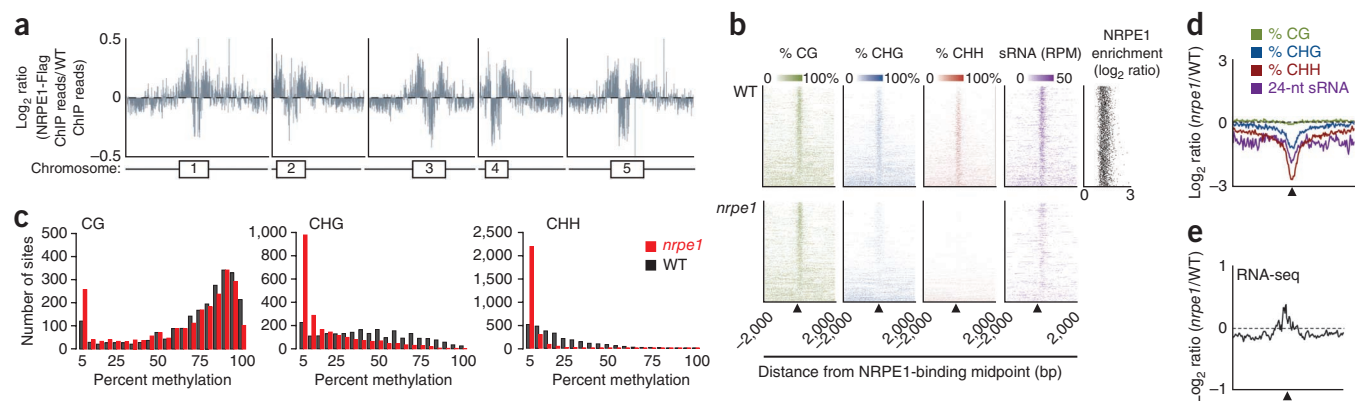


Figure 1 Identification of NRPE1-enriched sites by ChIP-seq and characterization of epigenetic marks at those sites. (a) Chromosomal view of NRPE1-Flag ChIP-seq reads relative to those for an untagged wild-type (WT) control, with a schematic representation of each chromosome shown below. The chromosome numbers represent the approximation of the centromere location, with the boxes indicating pericentromeric heterochromatin. (b) Heat maps showing the methylation levels in all three sequence contexts and 24-nt small RNA (sRNA) abundance (reads per base pair per million 21-nt mapping reads) for all NRPE1 sites ($\pm 2,000$ bp from midpoint) in wild type (top) and *nrpe1* mutants (bottom). Top right, scatter plot showing the relative NRPE1 enrichment at each site. (c) Distribution of the percent methylation of the central 100 base pairs of NRPE1 sites in wild type and *nrpe1* mutants. (d) Metaplot ($\pm 2,000$ base pairs from NRPE1-binding midpoints (triangle)) showing the relative change of epigenetic marks as in **b** for *nrpe1* mutants. (e) Metaplot showing the changes of RNA-seq reads in *nrpe1* mutants relative to wild type.

in two biological replicates (Supplementary Table 1). The vast majority of these defined NRPE1 binding regions (2,300 sites, or approximately 88%) were shorter than 250 base pairs (bp) (Supplementary Fig. 1), consistent with a recent finding that Pol V-dependent small RNAs are derived from small intergenic loci¹⁶. To examine the biological significance of these sites, we performed a series of genomic and epigenomic profiling experiments.

We first examined the role of NRPE1 in RdDM by performing whole-genome bisulfite sequencing and small-RNA sequencing in *nrpe1* mutant and wild-type plants. DNA methylation in all three sequence contexts (CG, CHG and CHH) was highly enriched at NRPE1 binding sites in wild-type (Fig. 1b). Notably, methylation of CHH and, to a lesser extent, CHG at these sites was NRPE1 dependent (Fig. 1b–d and Supplementary Fig. 2a). Genome-wide small-RNA profiling similarly identified a strong enrichment of NRPE1-dependent 24-nt

RNAs at NRPE1 binding sites (Fig. 1b,d and Supplementary Fig. 2b). We also analyzed a published RNA sequencing (RNA-seq) data set¹⁷ and found, consistent with the silencing function of RdDM, that RNA reads were elevated at NRPE1 binding regions in the *nrpe1* mutant relative to wild type (Fig. 1e). Thus, Pol V-bound sites are highly correlated with marks of epigenetic gene silencing as well as with the suppression of mRNA in those regions.

DDR complex is required for global Pol V chromatin association

To test the extent to which the DDR complex is required for Pol V localization to chromatin, we crossed the NRPE1-Flag transgene separately into the *drd1*, *dms3* and *rdm1* mutant backgrounds and profiled genome-wide occupancy of NRPE1 in these mutants and a replicate wild type by ChIP-seq. We found that *drd1*, *dms3* and *rdm1* mutations all strongly reduced or eliminated NRPE1 enrichment at all of the defined NRPE1 binding sites (Fig. 2a,b). These results suggest that the previously reported effects of *drd1*, *dms3* and *rdm1* mutations on Pol V transcript accumulation are due to changes in Pol V chromatin association. As NRPE1 protein levels were similar between wild-type and mutant plants

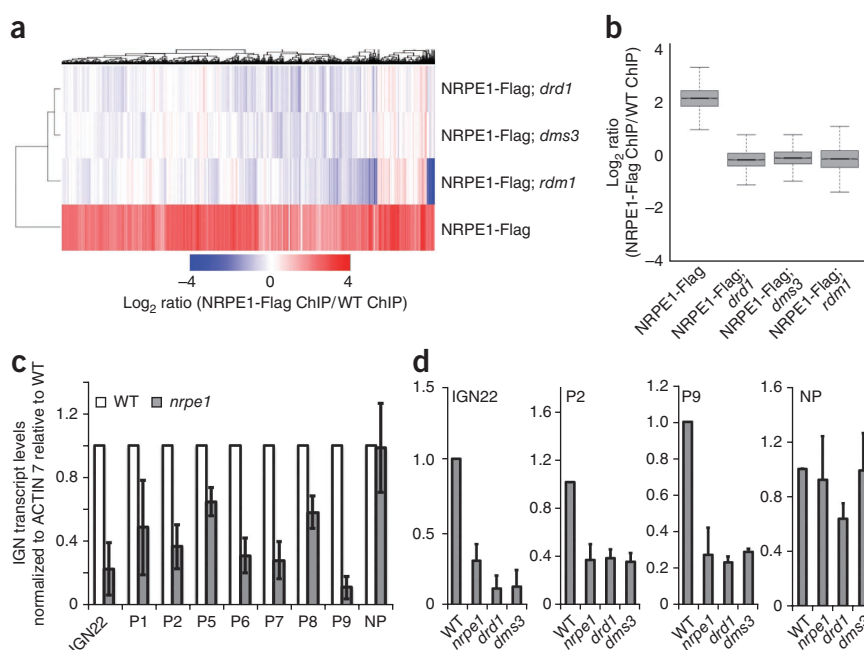
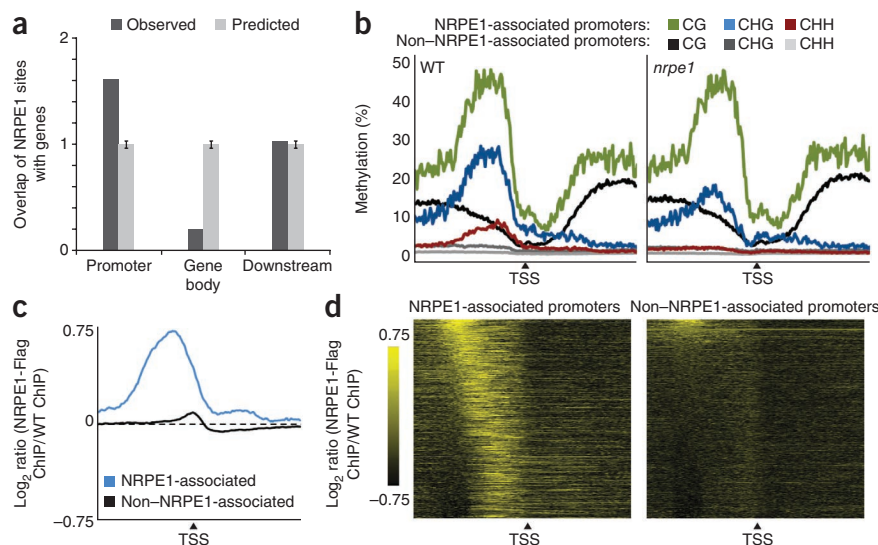


Figure 2 The DDR complex is required for stable association of Pol V with chromatin. (a) Heat map of NRPE1 enrichment at sites defined in ChIP-seq experiments in wild type and mutants. The genotype of each library is indicated at far right. (b) Box plot (whiskers extend to ± 1.5 interquartile range (IQR)) of NRPE1 enrichment at sites shown in **a** for various genotypes. (c) Real-time qPCR analysis of transcripts originating from NRPE1 enrichment sites. IGN22 is a previously published Pol V target, P1–P9 are newly identified Pol V binding sites and NP is a non-NRPE1 enrichment region. (d) Real-time qPCR analysis of transcripts originating from NRPE1 enrichment sites in *nrpe1*, *drd1* and *dms3* mutants. Error bars represent the s.d. of three biological replicates.

Figure 3 NRPE1 is enriched at gene promoters. (a) Relative enrichment of the observed overlap between NRPE1 sites and gene features compared to the average overlap of 10,000 genome-shuffling experiments. (b) Metaplots for wild-type and *nrpe1* genomes of DNA methylation for each cytosine context at NRPE1-associated promoters and non-NRPE1-associated promoters. (c,d) Metaplots (c) and heat maps (d) of ChIP-seq reads at NRPE1-associated promoters versus non-NRPE1-associated promoters. For each panel, black triangles denote the TSS, with plots extending $\pm 2,000$ bp upstream and downstream.



(Supplementary Fig. 3a), these results indicate that all members of the DDR complex act to promote stable genome-wide Pol V association with its chromatin targets, and they also further verify that our identified NRPE1 peaks are biologically significant.

Pol V sites correlate with NRPE1-dependent transcripts

Previous studies have identified several Pol V-dependent noncoding RNA transcripts^{5,13}. To explore whether our ChIP-seq data set would enable us to identify new Pol V-dependent transcripts, we tested for the presence of potential Pol V-dependent transcripts at our identified NRPE1-enrichment sites. Of seven randomly chosen and validated NRPE1-enrichment sites (Supplementary Fig. 3b,c), all showed the presence of detectable Pol V-dependent transcripts when assessed by quantitative real-time PCR (real-time qPCR) (Fig. 2c). In line with our ChIP-seq data, for those RNAs tested (Supplementary Fig. 3d), the Pol V-dependent transcripts were also DDR dependent (Fig. 2d).

Taken together, our ChIP-seq results, in conjunction with our epigenomic profiling of *nrpe1* mutants and the discovery of new Pol V-dependent transcripts, suggest that the enrichment sites in our ChIP-seq data set represent bona fide Pol V binding sites.

Pol V is enriched at gene promoters containing transposons

Next, we sought to identify common features of Pol V targets. Notably, yet perhaps consistently with its likely ancestral relationship to Pol II,

we found that NRPE1 sites are enriched at gene promoters, which we defined as sequences up to 1 kb upstream of a putative transcription start site (Fig. 3a). This observation was further supported by analysis of previously published histone-modification profiles¹⁸, in which we found that NRPE1 sites are flanked by histone H3 Lys4-methylation chromatin marks that are found near promoter and genic regions (Supplementary Fig. 4a)¹⁸. Promoters overlapping NRPE1 sites, which we refer to as 'NRPE1 associated,' are intrinsically different from non-NRPE1-associated promoters in that they contain much higher levels of DNA methylation and 24-nt small RNAs (Fig. 3b and Supplementary Fig. 4b). Notably, we found that even at promoters classified by our analysis as 'non-NRPE1 associated' there was a small enrichment of NRPE1 (Fig. 3c,d), suggesting that gene promoters may recruit Pol V in a weak and/or transient manner.

The epigenetic profile of NRPE1-associated promoters can be at least partially attributed to the fact that 55% of NRPE1-associated promoters overlapped with transposons (Fig. 4a), with transposon-proximal genes generally showing higher NRPE1 enrichment at their promoters than do genes far from transposons (Fig. 4b). As expected from the

presumed function of the RdDM pathway, a large number of the NRPE1 peaks mapped to annotated transposons (Fig. 4c). Further supporting the notion that Pol V might have an inherent affinity for promoters, we found that

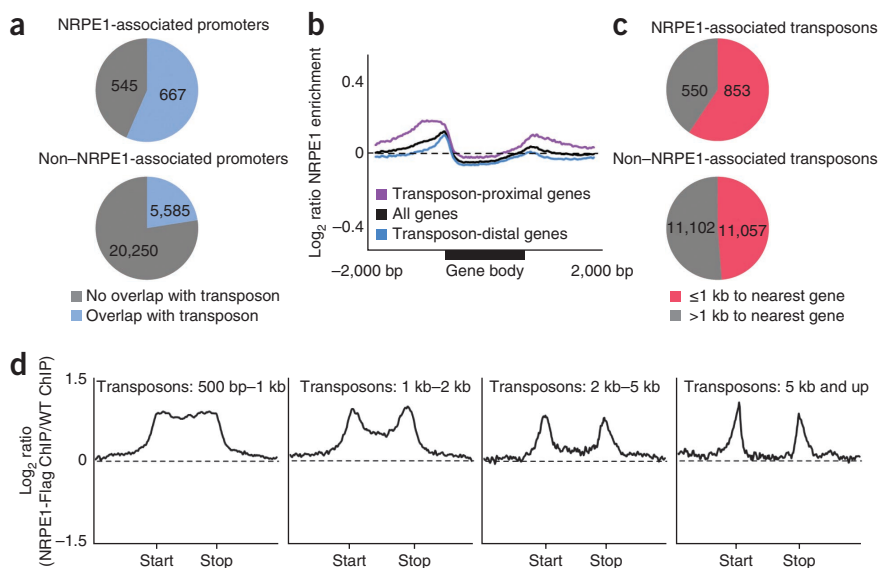


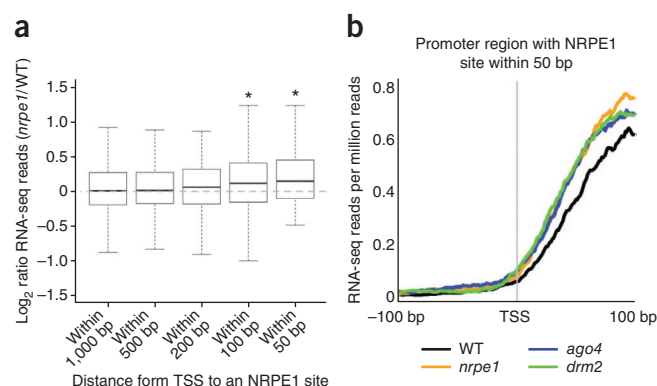
Figure 4 NRPE1 is enriched at the intersection of promoters and transposons. (a) NRPE1-associated promoters are enriched for promoters overlapping with transposons ($P < 2.2 \times 10^{-16}$, Fisher's exact test). (b) Metaplot showing NRPE1 enrichment at transposon-proximal (within 1 kb) and transposon-distal (>1 kb) protein-coding genes for $\pm 2,000$ bp upstream and downstream and over the gene body (shown in percent coverage of gene 5' to 3'). (c) NRPE1-associated transposons (those overlapping with an NRPE1 site) are enriched for gene-proximal transposons ($P < 2.2 \times 10^{-16}$, Fisher's exact test). (d) Metaplots of NRPE1 enrichment at NRPE1-associated transposons, organized by size class.

Figure 5 Loss of NRPE1 causes changes in protein-coding gene expression. (a) Box plots (whiskers extend ± 1.5 IQR) of \log_2 ratios of normalized RNA-seq read counts for *nrpe1* mutants to those for wild-type plants for protein-coding genes with an NRPE1 site in their promoter. Each box plot represents a subclass of those genes based on the distance between the TSS and the NRPE1 site. * $P < 0.05$ (Mann-Whitney test). (b) Metaplot showing the normalized RNA-seq reads for different RdDM mutants at and around the TSS of protein-coding genes with an NRPE1 site within 50 bp upstream of the TSS.

at NRPE1-associated transposons the profile of NRPE1 binding showed a clear enrichment at transposon edges (Fig. 4d), which are known to contain autonomous transposon promoter elements^{19,20}. Similarly to what we observed at NRPE1-associated promoters (Fig. 3b), the subset of transposons that are NRPE1 associated was significantly enriched for transposons within 1 kb of a protein-coding gene (Fig. 4c and Supplementary Fig. 5a,b), and these transposons were more heavily methylated and targeted by 24-nt small RNAs than were non-NRPE1-associated transposons (Supplementary Fig. 5c,d). Thus, our observation that a majority of NRPE1 sites (~54%) overlapped with transposons or transposon fragments within gene promoters supports prevailing models of RdDM, wherein repetitive elements such as transposons are common targets, but it also suggests that gene promoters, especially promoters with nearby transposons, are frequent targets of Pol V.

Loss of Pol V affects the transcription of Pol V-proximal genes

Given the association of Pol V with promoters, we sought to determine whether Pol V affects the transcription of endogenous protein-coding genes. We examined mRNA expression changes in *nrpe1* plants relative to wild-type plants for genes near NRPE1 sites. Indeed, we did observe a significant increase in mRNA expression at genes close to NRPE1 sites as compared to genes not close to NRPE1 sites. In particular, the nearer the NRPE1 site was to the predicted transcriptional start site (TSS), the larger the increase in expression (Fig. 5a). Thus, in the absence of Pol V function, genes near Pol V targets are upregulated. To test whether the upregulation is due to the production of alternative upstream transcripts that are derepressed in *nrpe1* mutant plants, or whether it is mainly restricted to the protein-coding gene transcripts, we mapped the RNA-seq reads relative to the transcriptional start sites. We found that the extra RNA-seq reads in *nrpe1* mutant plants mapped almost exclusively downstream of the TSS, suggesting that loss of Pol V causes upregulation of the main



Pol II protein-coding gene transcripts (Fig. 5b). One possibility is that the upregulation of genes in *nrpe1* mutant plants is due to the loss of Pol V transcripts, which otherwise interfere with the transcription of the Pol II promoter. Alternatively, the proximity of an NRPE1 site to a gene might increase the likelihood that RdDM will dampen the activity of the protein-coding gene promoter. To distinguish between these hypotheses, we analyzed RNA-seq data from two additional RdDM mutants, *drm2* and *ago4*, that act downstream of Pol V action^{5,13,15}. We observed a very similar pattern of gene upregulation at genes near the NRPE1 sites in these other RdDM mutants (Fig. 5b and Supplementary Fig. 4c,d), suggesting that loss of RdDM in general, rather than loss of Pol V specifically, is causing upregulation of normal Pol II initiation.

Pol V is enriched at evolutionarily recent transposons

Because Pol V only targets a subset of transposons in the genome (Fig. 4c), we sought to determine whether these transposons have any commonalities. In *A. thaliana*, gene-proximal transposons are relatively young compared to gene-distal transposons²¹. Given that NRPE1-associated transposons were enriched for gene-proximal transposons, we investigated the relative age of NRPE1-targeted transposons. For this analysis, we used the genome of a close *A. thaliana* relative, *Arabidopsis lyrata*²², to distinguish between transposons conserved in the two genomes ('ancient'; Supplementary Table 2) and those found only in *A. thaliana* ('unique'), which are therefore relatively young²¹. We found that NRPE1-associated transposons were enriched for unique transposons (Fig. 6a) and that NRPE1-associated promoters were similarly enriched for unique transposons (Fig. 6b). Moreover, when comparing unique versus ancient transposons,

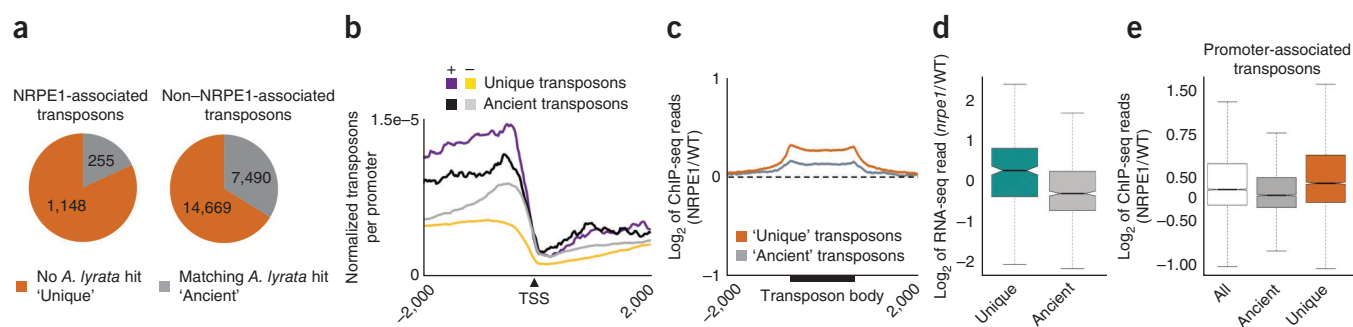


Figure 6 NRPE1 is enriched at transposons that are relatively new in the *A. thaliana* genome. (a) NRPE1-associated transposons are enriched for transposons unique to *A. thaliana* ($P < 2.2 \times 10^{-16}$, Fisher's exact test). (b) Relative transposon abundance (ratio of transposons per promoter to total number of transposons of that type) at NRPE1-associated (+) and non-NRPE1-associated (-) promoters. (c) Metaplot showing the ChIP-seq read ratios over unique and ancient transposons. (d) \log_2 ratio of RNA-seq reads in *nrpe1* mutants compared to wild type. (e) NRPE1 is significantly enriched at 'unique' transposons found at promoters as compared to either all promoter-associated transposons or 'ancient' promoter-associated transposons ($P < 2.2 \times 10^{-16}$, Mann-Whitney test).

irrespective of overlap with called NRPE1 peaks, we found that unique transposons showed a significant enrichment for NRPE1 binding (Fig. 6c; $P < 2.2 \times 10^{-16}$, Mann-Whitney test). We also noted that, whereas unique transposons were generally more weakly expressed than were ancient transposons (Supplementary Fig. 6), mutations in *NRPE1* resulted in greater gains of expression for unique transposons relative to ancient transposons (Fig. 6d). Although these results indicate that young transposons are a preferred target for NRPE1, it is also possible that this could also be an indirect effect of young transposons being gene proximal, as previously reported²¹. To control for this, we compared gene-proximal ancient transposons with gene-proximal unique transposons and found that, even among the gene-proximal subset, unique transposons were enriched for NRPE1 targets as compared to ancient transposons ($P < 2.2 \times 10^{-16}$, Fisher's exact test). In addition, NRPE1 itself was also enriched at gene-proximal unique transposons (Fig. 6e). These results suggest that transposon age may be a determinant of Pol V targeting and that RdDM could be an epigenetic readout of the evolutionary history of repetitive elements in the *Arabidopsis* genome.

DISCUSSION

In this study, we have generated the first genome-wide chromatin-association profile of an RdDM component. We believe that these data sets have identified bona fide Pol V sites that are biologically significant, because epigenomic profiling indicates that these are sites of NRPE1-dependent DNA methylation and small-RNA accumulation, consistent with the role of Pol V in RdDM. Additionally, the loss of NRPE1 chromatin association in mutants with disruption of the DDR putative chromatin-remodeling complex further confirms that the identified Pol V target sites are biologically significant.

The observation that Pol V is enriched at gene promoters is noteworthy. It suggests that although Pol V has evolved from the ancestral Pol II to target *de novo* DNA methylation, it may retain some Pol II binding preferences for gene-proximal regions. Consistent with this idea, even at promoters without defined NRPE1 peaks, we observed an enrichment of NRPE1 ChIP-seq reads near the transcriptional start site (Fig. 3c,d). This suggests that a broader set of promoters than those we have identified may be transient targets of Pol V, with more stable association occurring only at a subset of promoters.

The key determinants for a promoter region to become strongly associated with Pol V are unknown, but our data indicate that the presence of a transposable element, particularly a relatively young insertion, is a major driver in the stable association of Pol V to a given genomic locus. Thus, it appears that Pol V preferentially associates at regions where promoters and transposons overlap. This conclusion is further supported by the observation that younger transposons, which tend to be close to genes, are preferential targets of Pol V. Our analysis of RNA-seq data sets shows that the endogenous protein-coding genes near Pol V sites are upregulated upon loss of RdDM effectors, indicating that the active targeting of promoters and transposons by Pol V has functional implications for the transcriptome. Furthermore, the results provide a potential explanation for previous observations that genes near methylated transposons are often associated with reduced expression^{21,23}.

Given the observed pattern of Pol V association within the genome, it appears that Pol V transiently associates with most promoters. We hypothesize that when an active transposon jumps into a promoter region of a gene, Pol V will become more stably associated with that promoter and the associated transposon, thus targeting the transposon for *de novo* DNA methylation and transcriptional repression, preventing further movement of the transposon and potentially

mitigating the effects of the insertion on nearby genes. In this model, Pol V and RdDM have evolved to act in genome surveillance for newly inserted transposons, especially those near genes. The MET1 and CMT3 DNA methylation pathways would subsequently maintain epigenetic silencing of those targets. This idea is supported by the relatively greater loss of CHH methylation compared to CG and CHG DNA methylation in *nrpe1* mutants (Fig. 1c).

The results of Pol V ChIP-seq provide insights into the genome-wide targets of a noncanonical eukaryotic DNA-dependent RNA polymerase. In the future, it will be important to test whether the targeting of this polymerase is solely dictated by the genomic elements suggested by this study or if there are other chromatin-level or protein-interaction components that direct recruitment.

METHODS

Methods and any associated references are available in the online version of the paper.

Accession codes. Sequencing data were deposited at NCBI, with code GSE39247.

Note: Supplementary information is available in the online version of the paper.

ACKNOWLEDGMENTS

We thank T. Lagrange at the Université de Perpignan, Perpignan, France, for the NRPE1-Flag transgenic seeds and M. Akhavan for assistance with high-throughput sequencing. X.Z. is supported by Ruth L. Kirschstein National Research Service grant F32GM096483-01. C.J.H. is supported by the Damon Runyon Cancer Research Foundation fellowship. S.F. is supported by the Leukemia & Lymphoma Society Special fellowship. This work was supported by NIH grant GM60398, and S.E.J. is supported as an investigator of the Howard Hughes Medical Institute.

AUTHOR CONTRIBUTIONS

X.Z., C.J.H. and S.E.J. designed the experiments. X.Z., C.J.H., J.A.L., L.M.J., A.T. and S.F. performed the experiments. X.Z. and C.J.H. analyzed the data and wrote the manuscript.

COMPETING FINANCIAL INTERESTS

The authors declare no competing financial interests.

Published online at <http://www.nature.com/doi/10.1038/nsmb.2354>.

Reprints and permissions information is available online at <http://www.nature.com/reprints/index.html>.

1. Law, J.A. & Jacobsen, S.E. Establishing, maintaining and modifying DNA methylation patterns in plants and animals. *Nat. Rev. Genet.* **11**, 204–220 (2010).
2. Cokus, S.J. *et al.* Shotgun bisulphite sequencing of the *Arabidopsis* genome reveals DNA methylation patterning. *Nature* **452**, 215–219 (2008).
3. Haag, J.R. & Pikaard, C.S. Multisubunit RNA polymerases IV and V: purveyors of non-coding RNA for plant gene silencing. *Nat. Rev. Mol. Cell Biol.* **12**, 483–492 (2011).
4. Mosher, R.A., Schwach, F., Studholme, D. & Baulcombe, D.C. PolIVb influences RNA-directed DNA methylation independently of its role in siRNA biogenesis. *Proc. Natl. Acad. Sci. USA* **105**, 3145–3150 (2008).
5. Wierzbicki, A.T., Haag, J.R. & Pikaard, C.S. Noncoding transcription by RNA polymerase Pol IVb/Pol V mediates transcriptional silencing of overlapping and adjacent genes. *Cell* **135**, 635–648 (2008).
6. Kanno, T. *et al.* Involvement of putative SNF2 chromatin remodeling protein DRD1 in RNA-directed DNA methylation. *Curr. Biol.* **14**, 801–805 (2004).
7. Kanno, T. *et al.* A structural-maintenance-of-chromosomes hinge domain-containing protein is required for RNA-directed DNA methylation. *Nat. Genet.* **40**, 670–675 (2008).
8. Ausin, I., Mockler, T.C., Chory, J. & Jacobsen, S.E. IDN1 and IDN2 are required for *de novo* DNA methylation in *Arabidopsis thaliana*. *Nat. Struct. Mol. Biol.* **16**, 1325–1327 (2009).
9. Law, J.A. *et al.* A protein complex required for polymerase V transcripts and RNA-directed DNA methylation in *Arabidopsis*. *Curr. Biol.* **20**, 951–956 (2010).
10. Gao, Z. *et al.* An RNA polymerase II- and AGO4-associated protein acts in RNA-directed DNA methylation. *Nature* **465**, 106–109 (2010).
11. Zheng, B. *et al.* Intergenic transcription by RNA polymerase II coordinates Pol IV and Pol V in siRNA-directed transcriptional gene silencing in *Arabidopsis*. *Genes Dev.* **23**, 2850–2860 (2009).

12. El-Shami, M. *et al.* Reiterated WG/GW motifs form functionally and evolutionarily conserved ARGONAUTE-binding platforms in RNAi-related components. *Genes Dev.* **21**, 2539–2544 (2007).
13. Rowley, M.J., Avrutsky, M.I., Sifuentes, C.J., Pereira, L. & Wierzbicki, A.T. Independent chromatin binding of ARGONAUTE4 and SPT5L/KTF1 mediates transcriptional gene silencing. *PLoS Genet.* **7**, e1002120 (2011).
14. Huang, L. *et al.* An atypical RNA polymerase involved in RNA silencing shares small subunits with RNA polymerase II. *Nat. Struct. Mol. Biol.* **16**, 91–93 (2009).
15. Wierzbicki, A.T., Ream, T.S., Haag, J.R. & Pikaard, C.S. RNA polymerase V transcription guides ARGONAUTE4 to chromatin. *Nat. Genet.* **41**, 630–634 (2009).
16. Lee, T.F. *et al.* RNA polymerase V-dependent small RNAs in *Arabidopsis* originate from small, intergenic loci including most SINE repeats. *Epigenetics* **7**, 798–795 (2012).
17. Ausin, I. *et al.* An IDN2-containing complex involved in RNA-directed DNA methylation in *Arabidopsis*. *Proc. Natl. Acad. Sci. USA* **109**, 8374–8381 (2012).
18. Zhang, X., Bernatavichute, Y.V., Cokus, S., Pellegrini, M. & Jacobsen, S.E. Genome-wide analysis of mono-, di- and trimethylation of histone H3 lysine 4 in *Arabidopsis thaliana*. *Genome Biol.* **10**, R62 (2009).
19. Slotkin, R., Nuthikattu, S. & Jiang, N. The impact of transposable elements on gene and genome evolution, in *Plant Genome Diversity* Vol. 1 (ed. Wendel, J.F.) Ch. 3, 35–55 (Springer Wien, 2012).
20. Lisch, D. Epigenetic regulation of transposable elements in plants. *Annu. Rev. Plant Biol.* **60**, 43–66 (2009).
21. Hollister, J.D. & Gaut, B.S. Epigenetic silencing of transposable elements: a trade-off between reduced transposition and deleterious effects on neighboring gene expression. *Genome Res.* **19**, 1419–1428 (2009).
22. Hu, T.T. *et al.* The *Arabidopsis lyrata* genome sequence and the basis of rapid genome size change. *Nat. Genet.* **43**, 476–481 (2011).
23. Hollister, J.D. *et al.* Transposable elements and small RNAs contribute to gene expression divergence between *Arabidopsis thaliana* and *Arabidopsis lyrata*. *Proc. Natl. Acad. Sci. USA* **108**, 2322–2327 (2011).

ONLINE METHODS

Plant materials. NRPE1-Flag¹² transgenic plants and *nrpe1-12* (SALK_033852)²⁴, *nrpd1-4* (SALK_083051)²⁵, *drd1-6* (ref. 6) and *dms3-4* (ref. 8) mutant plants are in the *A. thaliana* Columbia ecotype. Mutant *rdm1-1* was identified from *ros1-1* background in C24 ecotype¹⁰. The NRPE1-Flag transgene was crossed into the *drd1-6*, *dms3-4* and *rdm1-1* mutant backgrounds.

ChIP and RNA analysis. Two grams of flower tissues were used for ChIP using a previously published protocol with minor modifications^{26,27}. Chromatin was sonicated in a Bioruptor (Diagenode) for 15 min of 30 s on and 30 s off, and the chromatin was immunoprecipitated with anti-Flag M2 magnetic beads (Sigma). The enriched DNA was ethanol precipitated and subjected to library generation following Illumina's manufacturer instructions. ChIP-seq data were validated by independent ChIP experiments at nine randomly selected regions (P1–P9) as well as one NP region, located between two adjacent binding peaks, that served as a negative control. Only primers producing single amplification products were included for the validation analysis. Of these, regions P2 and P9 were selected as representative examples of typical NRPE1 occupancy in *drd1*, *dms3* and *rdm1* mutants. The data presented are relative to input (% input). Total RNA was isolated from flowers using TRIzol reagent (Invitrogen) and used to synthesize first-strand cDNA using SuperScript III (Invitrogen). Real-time qPCR was performed using the SYBR Green SuperMix (Bio-Rad) in a MxPro3000 qPCR machine (Stratagene), following the manufacturer instructions. The primers used are listed in **Supplementary Table 3**.

ChIP-seq, BS-seq and smRNA-seq library constructions and sequencing. Small RNA was extracted and purified from floral tissue as described²⁸. Libraries for ChIP-seq were generated using paired-end reagents from NEB and adapters from Illumina, and smRNA-seq libraries were generated using the Illumina True-seq protocol. BS-seq libraries were generated as previously reported². All libraries were sequenced at a length of 50 bp, using the HiSeq 2,000 platform and following manufacturer instructions (Illumina). Read statistics are listed in **Supplementary Table 4**.

Data analyses. Sequenced reads were base-called using the standard Illumina pipeline. For ChIP-seq and BS-seq libraries, only full 50-nt reads were retained, whereas for smRNA-seq libraries reads had the adaptor sequence trimmed and were retained if they were between 15 nt and 30 nt in length. For ChIP-seq and smRNA-seq libraries, reads were mapped to the *Arabidopsis* genome (TAIR8; <http://www.arabidopsis.org>) with Bowtie²⁹, allowing up to two mismatches and retaining only reads mapping uniquely to the genome for further analysis. For the biological replicate of the ChIP-seq experiment and the ChIP-seq of DDR mutants, 50,000,000 reads from the approximately 200,000,000 initial reads were taken as a subset for further analysis, in the interest of computational time. For BS-seq libraries, reads were mapped using the BSseeker wrapper for Bowtie³⁰. For ChIP-seq and BS-seq, identical reads were collapsed into one read, whereas for smRNA-seq identical reads were retained.

For methylation analysis, percent methylation was calculated as previously reported², with only cytosines having at least 5× coverage in both the

wild-type and *nrpe1* libraries included in any analysis. For all libraries, the list of mRNA and transposons along with genomic coordinates was obtained from TAIR (TAIR8). For all analyses, only transposons greater than 100 bp in length were used.

For analysis of the previously published mRNA-seq data sets¹⁷, we considered TAIR8 representative gene models within a given distance of an NRPE1 site, as described in the main text. To quantify expression change, we only considered genes that had at least ten reads in any of the libraries considered (Col, *ago4*, *drm2* or *nrpe1*), to filter out genes not expressed in the tissue considered.

Identification of NRPE1 peaks and calling of promoter and transposon overlaps. The R package BayesPeak^{31,32} was used to identify regions of NRPE1 enrichment in our NRPE1-Flag ChIP-seq library as compared to the Col ChIP-seq control library. To filter out false positives, we also identified peaks using a sliding-window approach by using a 200-bp window at 50-bp increments and performing a Fisher's-exact-test comparison between the ChIP-seq libraries. Resulting *P* values were Benjamini-Hochberg adjusted to estimate FDRs. Only high-scoring peaks that overlapped from the Bayesian analysis (PP > 0.99999) and the Fisher test (FDR < 1 × 10^{−5}) were retained.

For the purposes of this study, 'overlap' of NRPE1 peaks with genomic regions (promoters/transposons) is called when ≥ 1 bp of a peak overlaps with a locus. Similarly, elements were considered 'proximal' if within 1 kb of each other, and 'distal' if farther than 1 kb from each other.

Classification of 'ancient' versus 'unique' transposons. The list of TAIR8 transposable elements (ftp://ftp.arabidopsis.org/home/tair/Genes/TAIR8_genome_release/TAIR8_Transposable_Elements.txt) were classified as either 'unique' or 'ancient', using the exact methodology previously described²¹. The *A. lyrata* genome (Araly1, unmasked) was downloaded from JGI (<http://genome.jgi-psf.org/Araly1/Araly1.home.html>) and used to generate a BLAST database.

24. Pontier, D. *et al.* Reinforcement of silencing at transposons and highly repeated sequences requires the concerted action of two distinct RNA polymerases IV in *Arabidopsis*. *Genes Dev.* **19**, 2030–2040 (2005).
25. Herr, A.J., Jensen, M.B., Dalmay, T. & Baulcombe, D.C. RNA polymerase IV directs silencing of endogenous DNA. *Science* **308**, 118–120 (2005).
26. Johnson, L., Cao, X. & Jacobsen, S. Interplay between two epigenetic marks. DNA methylation and histone H3 lysine 9 methylation. *Curr. Biol.* **12**, 1360–1367 (2002).
27. Stroud, H. *et al.* Genome-wide analysis of histone H3.1 and H3.3 variants in *Arabidopsis thaliana*. *Proc. Natl. Acad. Sci. USA* **109**, 5370–5375 (2012).
28. Lu, C., Meyers, B.C. & Green, P.J. Construction of small RNA cDNA libraries for deep sequencing. *Methods* **43**, 110–117 (2007).
29. Langmead, B., Trapnell, C., Pop, M. & Salzberg, S.L. Ultrafast and memory-efficient alignment of short DNA sequences to the human genome. *Genome Biol.* **10**, R25 (2009).
30. Chen, P.Y., Cokus, S.J. & Pellegrini, M.B.S. Seeker: precise mapping for bisulfite sequencing. *BMC Bioinformatics* **11**, 203 (2010).
31. Spyrou, C., Stark, R., Lynch, A.G. & Tavare, S. BayesPeak: Bayesian analysis of ChIP-seq data. *BMC Bioinformatics* **10**, 299 (2009).
32. Cairns, J. *et al.* BayesPeak—an R package for analysing ChIP-seq data. *Bioinformatics* **27**, 713–714 (2011).